Effect of stacking fault energy on strength and ductility of nanostructured alloys: An evaluation with minimum solution hardening

Pei-Ling Sun [a,*], Y.H. Zhao [b], J.C. Cooley [c], M.E. Kassner [d], Z. Horita [e], T.G. Langdon [d,f], E.J. Lavernia [b], Y.T. Zhu [g]

[a] Department of Materials Science and Engineering, Feng Chia University, Taichung 407, Taiwan
[b] Department of Chemical Engineering and Materials Science, University of California, Davis, CA 95616, USA
[c] Los Alamos National Laboratory, Los Alamos, NM 87545, USA
[d] Department of Aerospace & Mechanical Engineering, University of Southern California, Los Angeles, CA 90089-1453, USA
[e] Department of Materials Science & Engineering, Faculty of Engineering, Kyushu University, Fukuoka 819-0395, Japan
[f] Materials Research Group, School of Engineering Sciences, University of Southampton, Southampton SO17 1BJ, UK
[g] Department of Materials Science and Engineering, North Carolina State University, Raleigh, NC 27695, USA

ARTICLE INFO

ABSTRACT

The effect of stacking fault energy (SFE) on the mechanical properties was investigated in Ni–Co alloys which have minimum solution hardening effects. Cobalt reduces the SFE in nickel and this promotes grain refinement during processing and increases the dislocation and twin densities. A reduction in SFE increases strength and tensile ductility. The higher strength is due to grain refinement and higher dislocation and pre-existing twin densities whereas the higher ductility is attributed to a higher work hardening rate.

© 2009 Elsevier B.V. All rights reserved.

1. Introduction

The development of severe plastic deformation (SPD) technologies in the past decade has enabled the production of ultrafine-grained (UFG) metals in bulk form [1]. These UFG metals are fully dense and contamination-free so that they are ideal candidate materials for investigating the fundamental mechanisms and physical behavior of refined microstructures. It has been widely reported that the strength increases but the tensile ductility is sacrificed in many UFG materials [2–8], thereby limiting their industrial applications. Recently, substantial effort has been devoted to improve the poor tensile ductility of UFG materials [2,3,5,6,8–15].

The low tensile ductility in UFG materials is often attributed to their premature geometric instability (necking) which is a consequence of their low strain hardening. Strain hardening results typically from the accumulation of dislocations [16]. Large grains may have sufficient space within the grains for significant numbers of dislocations to intersect/tangle with each other and, consequently, to accumulate during deformation. However, in UFG materials the dislocations may no longer accumulate inside grains so that the grain interior is often relatively dislocation-free [17–19]. Thus, dislocations are often emitted from a grain boundary segment and deposited directly on other boundary segments with minimal dislocation accumulation and strain hardening in UFG metals. It has been shown that enhanced tensile ductility may be achieved in UFG materials through the use of various procedures such as a bi-modal grain size distribution [2,3], nanotwins [5], boundary structure engineering [6,9,13,15] and second phase precipitation [12,14,20]. However, these approaches often trade the increase in tensile ductility with a corresponding decrease in strength.

Recently, an investigation of the effect of stacking fault energy (SFE) on the mechanical behavior of UFG Cu–Zn alloys showed that a reduction in SFE may simultaneously increase both the tensile stress and the ductility [21]. This effect was attributed to the activation of both deformation twins and pre-existing twins due to processing by high-pressure torsion (HPT). Both the dislocation density and the twin density were reported to increase during the tensile testing. However, the presence of Zn in the alloys leads to significant solution hardening while also lowering the SFE and this

* Corresponding author. Tel.: +886 4 24517250x5345; fax: +886 4 24510014.
E-mail address: plsun@fcu.edu.tw (P.-L. Sun).

makes it difficult to specifically isolate the role played by the low SFE on the increase in strength. In practice, Co and Ni elements have similar atomic diameters [22] and it is known that their alloys experience very limited solution hardening [23,24]. Therefore, Ni–Co alloys are ideal candidate materials for clarifying this issue. In this study, nanostructured Ni–Co alloys processed by HPT and rolling were used to study the effect of SFE on the mechanical properties.

2. Experimental

Two Ni–Co alloys were produced by induction melting from Co and Ni pellets to give compositions of Ni–40 wt.% Co and Ni–65 wt.% Co. These two alloys form fcc solid solutions. It is well established that the addition of cobalt reduces the SFE of the alloy. Using a detailed compilation of SFE data for various Ni–Co alloys, which are plotted to give a line of best fit [25], the SFE were estimated as ~100 and ~20 mJ/m^2 for the Ni–40 wt.% Co alloy and Ni–65 wt.% Co alloys, respectively. The estimated difference in the SFE for the two alloys by a factor of ~5 is consistent with the data available from embedded-atom calculations [26]. The as-cast alloys were machined into discs of 1 mm in thickness and 10 mm in diameter and these discs were processed by HPT at room temperature to a total of 5 revolutions at 1 rpm under an applied pressure of 6.0 GPa. Following HPT, the discs were cold-rolled at ambient temperature to thin ribbons with a thickness of 0.2 mm corresponding to a rolling reduction of 80%.

Transmission electron microscopy (TEM) samples were prepared from the as-deformed specimens by mechanically grinding samples to a thickness of ~80 μm and with a final thinning by Ar$^+$ ion milling at 4 keV ion energy. The microstructures were characterized using a Philips CM200 transmission electron microscope at 200 kV. Dark-field images were employed to determine the grain sizes. Selected area electron diffraction (SAED) patterns were also recorded in both alloys and these patterns were used to determine the misorientation angles of the grain boundaries.

X-ray diffraction (XRD) measurements were performed using Cu K$_\alpha$ radiation to estimate the dislocation densities. The θ–2θ scans were performed at room temperature at a scan rate of 1°/min. Pure Al annealed at 400 °C was used as an XRD peak-broadening reference for both the grain size and the microstrain calculations. The peak parameters, including the peak intensity, the peak-maximum position, the full-width half-maximum and the integral breadth, were determined using Microcal (TM) Origin® by fitting a Lorentzian function to the measured peaks. The entire tensile specimens were scanned for the XRD analysis.

Tensile test samples were machined from the cold-rolled specimens to a gauge length of 10 mm, a width of 2 mm and a thickness of 0.2 mm. Uniaxial tensile tests were performed on the samples with an initial strain rate of 1.0×10^{-4}/s at 298 K. The strain was measured from the cross-head displacement without correction for the compliance. To minimize errors, duplicate tests were also conducted.

3. Results and discussion

Typical microstructures in the two as-processed alloys are shown in Fig. 1. Both samples have diffuse microstructures in the TEM indicative of high dislocation densities. An extensive examination of the microstructures showed the majority of grains are equiaxed and twins are present in the grain interiors of both alloys. An example of a twin is labeled in Fig. 1(b). Using dark-field TEM, the average grain sizes were estimated as ~85 and ~115 nm for the Ni–65 wt.% Co alloy and the Ni–40 wt.% Co alloy, respectively. The SAED patterns, taken from areas of ~0.8 μm^2, show rings thereby
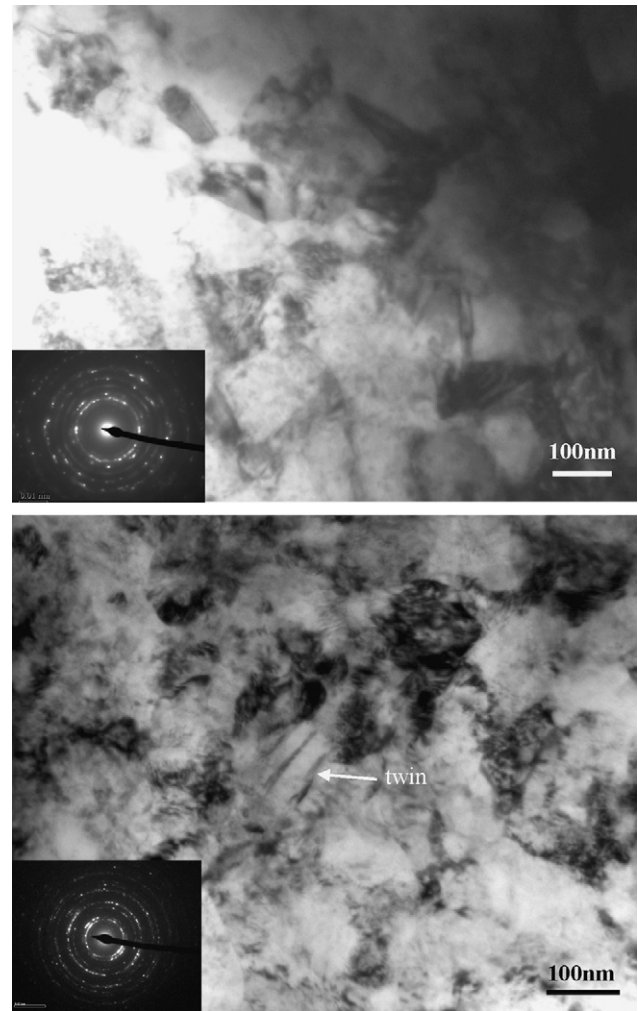

Fig. 1. The as-deformed microstructure and SAED patterns of (a) Ni–40 wt.% Co alloy and (b) Ni–65 wt.% Co alloy.

suggesting that most of the grain boundaries within these areas have high angles of misorientation.

The engineering stress–strain curves of the two samples are shown in Fig. 2. It can be seen that the Ni–65 wt.% Co alloy has higher yield and ultimate tensile strengths than the Ni–40 wt.% Co alloy. The Ni–65 wt.% Co alloy also exhibits a higher normalized
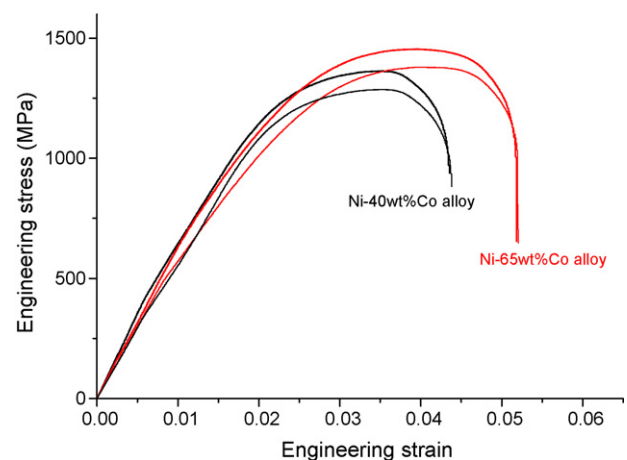

Fig. 2. Engineering stress–strain curves for both Ni–40 wt.% Co alloy and Ni–65 wt.% Co alloy.
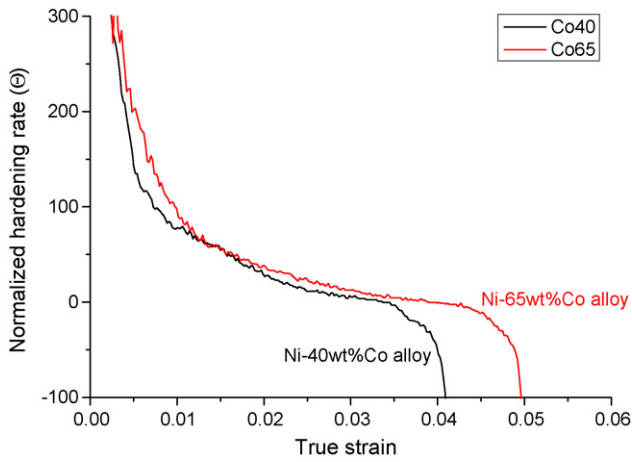
Fig. 3. The normalized work hardening rate versus the true strain for both Ni–40 wt.% Co alloy and Ni–65 wt.% Co alloy.
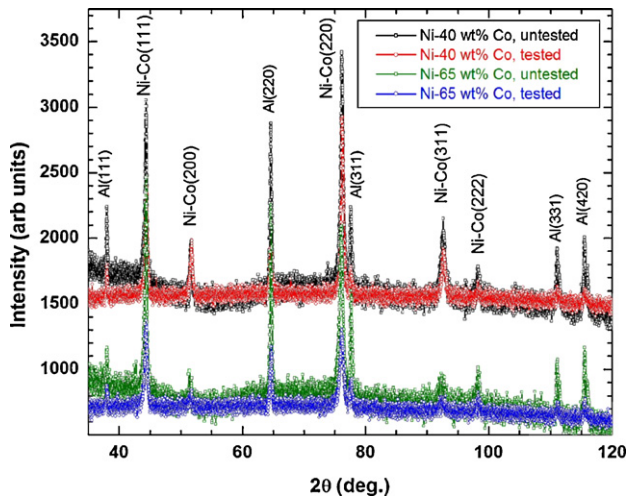

Fig. 4. The XRD patterns of as-deformed (untested) and tensile tested (tested) samples. The peaks become broader after tensile test for both samples, indicating the increase in defect density (dislocation and twin).

work hardening rate (Θ), which extends to higher strains than in the Ni–40 wt.% Co alloy (Fig. 3). Θ is defined by $\Theta = 1/\sigma(\partial\sigma/\partial\varepsilon)\varepsilon$, where σ is true stress and ε is true strain. The elongation to failure was also measured from the broken samples after the tensile testing. The average elongation to failure is 2.8% in the Ni–40 wt.% Co alloy and 3.6% in the Ni–65 wt.% Co alloy. The mechanism responsible for the stronger strain hardening in samples with lower SFE was investigated by XRD analyses of the samples before and after tensile testing. The XRD patterns of these samples are shown in Fig. 4 where the Al peaks are from the fixtures. It is apparent that the XRD peaks of both samples become broadened after tensile testing which is indicative of an increase in the density of lattice imperfections such as dislocations and twins. In addition, the Ni–65 wt.% Co alloy has broader peaks than the Ni–40 wt.% Co alloy. By using the Williamson–Hall integral-breadth method [27], it was possi-

ble to estimate the microstrain and hence the dislocation density [28,29]. The results are given in Table 1 and it can be seen that the dislocation densities of both alloys increase during tensile testing. This increase is by ~20% from $5.4 \times 10^{14}/m^2$ to $6.5 \times 10^{14}/m^2$ in the Ni–40 wt.% Co alloy and by ~50% from $6.5 \times 10^{14}/m^2$ to $9.8 \times 10^{14}/m^2$ in the Ni–65 wt.% Co alloy. It is concluded that the lower SFE in the Ni–65 wt.% Co alloy leads to a more efficient accumulation of dislocations and this contributes significantly to the higher strain hardening rate (Fig. 3).

It should be noted also that the XRD analysis provides only qualitative estimates of the dislocation densities and not a direct measure of the absolute values. For example, different XRD analyses may yield values for the dislocation densities that vary by an order of magnitude in similar samples [21,30]. Nevertheless, it is well established that the relative dislocation densities can be compared for different materials if they are measured and calculated using the same experimental method. Accordingly, the relative change in dislocation density recorded in Table 1 before and after tensile testing corresponds to a valid trend for these two alloys.

Another significant factor that may affect the strain hardening rate is the twin accumulation during tensile testing. The twin density, β, defined as the probability of finding a twin boundary between any two neighboring {1 1 1} planes, was calculated using the expression [31,32]:

$$\beta = \frac{\Delta C.G.(2\theta)_{111} - \Delta C.G.(2\theta)_{200}}{11 \tan \theta_{111} + 14.6 \tan \theta_{200}} \tag{1}$$

where $\Delta C.G.(2\theta)_{111}$ and $\Delta C.G.(2\theta)_{200}$ are the angular deviations of the gravity center from the peak maximum of the {1 1 1} and {2 0 0} XRD peaks, respectively. It was found that the twin density increased after tensile testing in both alloys indicating an accumulation of twins during the tensile testing. It is evident from Table 1 that the twin density increments are similar in both alloys. These observations show, therefore, that the higher work hardening rate in the Ni–65 wt.% Co alloy is primarily derived from the higher accumulation of dislocations.

The experimental results in this study provide a clearly demonstration that by lowering the SFE, in the absence of any significant solution hardening, can simultaneously increase both the strength and the ductility of nanostructured materials. The increase in strength is derived from a smaller grain size, a higher twin density and a higher dislocation density in the Ni–65 wt.% Co alloy where the SFE is low by comparison with the Ni–40 wt.% Co alloy. The increase in tensile ductility is primarily caused by the higher dislocation accumulation in the Ni–65 wt.% Co alloy due to the higher initial twin density, which leads to a higher work hardening rate during tensile testing. It has been reported that a high density of initial pre-existing twins can produce both high strength and high ductility [33,34]. This is because twins act as effective barriers that block the slipping dislocations and force them to accumulate on and near the twin boundaries. It should be noted that the enhancement in tensile ductility remains fairly limited in this study and this suggests that it may be effective to combine the present approach with other ductility-enhancing approaches such as lowering the initial dislocation density.

It is noted that deformation twinning was activated in both alloys during tensile testing in this investigation. At present it is not clear why the relative increases in twin densities are similar

Table 1
Grain size, dislocation density and twin density of the Ni–Co alloys.

	Grain size (nm), TEM	As-processed by HPT + rolling		After tensile testing	
		Dislocation density (1/m²)	Twin density (%)	Dislocation density (1/m²)	Twin density (%)
Ni–40 wt.% Co	115	5.4×10^{14}	0.9%	6.5×10^{14}	1.3%
Ni–65 wt.% Co	85	6.5×10^{14}	2.1%	9.8×10^{14}	3.0%

for both alloys but they are expected to increase the work hardening rates in these two alloys [21]. An optimum SFE was reported recently that produces the highest ductility in the Cu–Zn alloy system [35]. Further work is now required to determine whether there exists a similar optimum SFE in the Co–Ni alloy system.

4. Summary

This investigation evaluates the effect of SFE on the mechanical behavior and microstructure of nanostructured Co–Ni alloys without introducing, as in the Cu–Zn system, any additional complications that may arise from solution hardening. It is shown that a lower SFE leads to a smaller grain size and an increase in the densities of dislocations and deformation twins. In addition, a lower SFE simultaneously increases the strength and tensile ductility. The higher tensile strength is facilitated by the smaller grain size, higher dislocation density and higher density of twins formed during HPT. The improved ductility in tensile testing is attributed to the improved dislocation accumulation and higher rate of strain hardening.

Acknowledgements

References

[1] R.Z. Valiev, Y. Estrin, Z. Horita, T.G. Langdon, M.J. Zehetbauer, Y.T. Zhu, JOM 58 (4) (2006) 33–39.
[2] V.L. Tellkamp, A. Melmed, E.J. Lavernia, Metall. Mater. Trans. A 32 (2001) 2335–2343.
[3] Y. Wang, M.W. Chen, F.H. Zhou, E. Ma, Nature 419 (2002) 912–915.
[4] S. Cheng, J.A. Spencer, W.W. Milligan, Acta Mater. 51 (2003) 4505–4518.
[5] Y. Wang, E. Ma, Acta Mater. 52 (2004) 1699–1709.
[6] P.L. Sun, C.Y. Yu, P.W. Kao, C.P. Chang, Scripta Mater. 52 (2005) 265–269.
[7] C.Y. Yu, P.L. Sun, P.W. Kao, C.P. Chang, Scripta Mater. 52 (2005) 359–363.
[8] P.C. Hung, P.L. Sun, C.Y. Yu, P.W. Kao, C.P. Chang, Scripta Mater. 53 (2005) 647–652.
[9] L. Lu, L.B. Wang, B.Z. Ding, K. Lu, J. Mater. Res. 14 (2000) 270–273.
[10] R.K. Islamgaliev, N.F. Yunusova, I.N. Sabirov, A.V. Sergueeva, R.Z. Valiev, Mater. Sci. Eng. A 319–321 (2001) 877–881.
[11] R.Z. Valiev, I.V. Alexandrov, Y.T. Zhu, T.C. Lowe, J. Mater. Res. 17 (2002) 5–8.
[12] Z. Horita, K. Ohashi, T. Fujita, K. Kaneko, T.G. Langdon, Adv. Mater. 17 (2005) 1599–1602.
[13] P.L. Sun, E.K. Cerreta, G.T. Gray III, P. Rae, Mater. Sci. Eng. A 410–411 (2005) 265–268.
[14] S. Cheng, Y.H. Zhao, Y.T. Zhu, E. Ma, Acta Mater. 55 (2007) 5822–5832.
[15] P.L. Sun, E.K. Cerreta, J.F. Bingert, G.T. Gray III, M.F. Hundley, Mater. Sci. Eng. A 464 (2007) 343–350.
[16] U.F. Kocks, H. Mecking, Prog. Mater. Sci. 48 (2003) 171–273.
[17] C.P. Chang, P.L. Sun, P.W. Kao, Acta Mater. 48 (2000) 3377–3385.
[18] Y.T. Zhu, Y.R. Kobolov, G.P. Grabovetskaya, V.V. Stolyarov, N.V. Girsova, R.Z. Valiev, J. Mater. Res. 18 (2003) 1011–1016.
[19] P.L. Sun, E.K. Cerreta, G.T. Gray III, J.F. Bingert, Metall. Mater. Trans. A 37 (2006) 2983–2994.
[20] Y.H. Zhao, X.Z. Liao, S. Cheng, E. Ma, Y.T. Zhu, Adv. Mater. 18 (2006) 2280–2283.
[21] Y.H. Zhao, Y.T. Zhu, X.Z. Liao, Z. Horita, T.G. Langdon, Appl. Phys. Lett. 89 (2006) 121906.
[22] G.W.C. Kaye, T.H. Laby, Tables of Physical and Chemical Constants, 15th ed., Longman, London, UK, 1993.
[23] D.A. Hughes, W.D. Nix, Metall. Trans. A 19 (1988) 3013–3024.
[24] E. Wakai, T. Ezawa, T. Takenaka, J. Imamura, T. Tanabe, R. Oshima, J. Nuclear Mater. 367–370 (2007) 478–482.
[25] D.K. Chaudhuri, D. Xie, A.N. Lakshmanan, Wear 209 (1997) 140–152.
[26] X. Nie, R. Wang, Y. Ye, Y. Zhou, D. Wang, Solid State Commun. 96 (1995) 729–734.
[27] G.K. Williamson, W.H. Hall, Acta Metall. 1 (1953) 22–31.
[28] G.K. Williamson, R.E. Smallman, Philos. Mag. 1 (1956) 34–46.
[29] R.E. Smallman, K.H. Westmacott, Philos. Mag. 2 (1957) 669–683.
[30] L. Balogh, T. Ungár, Y.H. Zhao, Y.T. Zhu, Z. Horita, C. Xu, T.G. Langdon, Acta Mater. 56 (2008) 809–820.
[31] C.N.J. Wagner, Acta Metall. 5 (1957) 427–434.
[32] J.B. Cohen, C.N.J. Wagner, J. Appl. Phys. 33 (1962) 2073–2077.
[33] L. Lu, Y. Shen, X. Chen, L. Qian, K. Lu, Science 304 (2004) 422–426.
[34] Y.H. Zhao, J.F. Bingert, X.Z. Liao, B.Z. Cui, K. Han, A.V. Sergueeva, A.K. Mukherjee, R.Z. Valiev, T.G. Langdon, Y.T. Zhu, Adv. Mater. 18 (2006) 2949–2953.
[35] Y.H. Zhao, X.Z. Liao, Z. Horita, T.G. Langdon, Y.T. Zhu, Mater. Sci. Eng. A 493 (2008) 123–129.